Optimization of 3J IMM Solar Cells

Cooperative Research and Development Final Report

CRADA Number: CRD-17-704

NREL Technical Contact: Ryan France

NREL is a national laboratory of the U.S. Department of Energy
Office of Energy Efficiency & Renewable Energy
Operated by the Alliance for Sustainable Energy, LLC

This report is available at no cost from the National Renewable Energy Laboratory (NREL) at www.nrel.gov/publications.

Contract No. DE-AC36-08GO28308

Technical Report
NREL/TP-5900-72540
October 2018

Optimization of 3J IMM Solar Cells

Cooperative Research and Development Final Report

CRADA Number: CRD-17-704

NREL Technical Contact: Ryan France

NREL is a national laboratory of the U.S. Department of Energy
Office of Energy Efficiency & Renewable Energy
Operated by the Alliance for Sustainable Energy, LLC

This report is available at no cost from the National Renewable Energy Laboratory (NREL) at www.nrel.gov/publications.

Contract No. DE-AC36-08GO28308

Technical Report
NREL/TP-5900-72540
October 2018

National Renewable Energy Laboratory
15013 Denver West Parkway
Golden, CO 80401
303-275-3000 • www.nrel.gov

NOTICE

This work was authored by the National Renewable Energy Laboratory, operated by Alliance for Sustainable Energy, LLC, for the U.S. Department of Energy (DOE) under Contract No. DE-AC36-08GO28308. Funding provided by U.S. Department of Energy Office of Energy Efficiency and Renewable Energy Solar Energy Technologies Office. The views expressed herein do not necessarily represent the views of the DOE or the U.S. Government.

Cooperative Research and Development Final Report

In accordance with requirements set forth in the terms of the CRADA agreement, this document is the final CRADA report, including a list of subject inventions, to be forwarded to the DOE Office of Science and Technical Information as part of the commitment to the public to demonstrate results of federally funded research.

Parties to the Agreement: California Institute of Technology (CalTech)

CRADA number: CRD-17-704

CRADA Title: Optimization of 3J IMM Solar Cells

Joint Work Statement Funding Table showing DOE commitment: No DOE funding

Estimated Costs	NREL Shared Resources a/k/a Government In-Kind
Year 1	$ 00.00
TOTALS	$ 00.00

Abstract of CRADA Work:

Caltech is developing a lightweight concentrator photovoltaic system for space applications. The III-V group at the National Renewable Energy Laboratory (NREL) will collaborate with and assist Caltech by developing and optimizing 3-junction inverted metamorphic (3J IMM) solar cells grown by OMVPE for use in their space concentrator design.

Summary of Research Results:

The major project results were the modeling, development, and characterization of a 3-junction IMM device for the environment of CalTech's solar concentrator system, and providing material for creation of a concentrator prototype, radiation testing, and processing on thin glass and Kapton tape at CalTech for demonstration of very high specific power. The radiation tolerance of the 3J-IMM developed in this project was compared with a commercial 3J and found to be similar. A more radiation tolerant 3J-IMM device was envisioned using a novel GaInAsP alloy, and initial devices were developed, grown and characterized. In addition, a 4-junction IMM device grown and characterized, which targets the higher voltage demanded by the CalTech power transmission system. One manuscript is submitted and under review at J. Photovoltaics, including NREL contributions, and a presentation was given at the WCPEC-7.

Major Project Conclusions

- 3J-IMM samples were easily tuned for the CalTech system operating conditions (AM0 spectra, 15 suns, and 80 °C) while maintaining excellent performance. 24% efficiency is measured at 15 suns and 80 °C without an ARC, and 33% efficiency is modeled under the CalTech optics and with ARC.
- 3J-IMM cells were processed onto glass and Kapton tape with minimal loss at CalTech. The weight of the 3J-IMM solar cells is 2.2 mg compared to 15.2 mg for a commercial 3J, making the 3J-IMM higher efficiency and lower weight.
- Standard 3J-IMM cells have radiation hardness similar to commercial 3J devices.
- 1.0 eV GaInAsP with 25% phosphorus, a potentially radiation hard alloy, has a bandgap-voltage difference Woc = 0.4 V, similar to 1.0 eV GaInAs, despite having higher lattice-mismatch and being a quaternary alloy.
- Radiation hard 3J-IMM cells with 1.0 eV GaInAsP bottom subcells perform well and have no indication of loss associated with the GaInAsP alloy at BOL. The first device had over 20% at 1-sun AM0, 25°C, and without ARC.
- 4J-IMM cells achieved 23.9% at 1 sun AM0 while achieving the higher voltage, 3.345 V, demanded by the CalTech power transmission system, making it an excellent option for future PV devices in the CalTech system.
- 3J-IMM and 4J-IMM devices showed no unexpected losses at elevated temperature and concentration.

Summary of project work at NREL

- Modeled 3J performance and optimal bandgap combinations for various temperatures and concentrations, and for the specific system envisioned in the space solar concentrator system
- Taught inverted device processing to CalTech during a 3-day site visit, including growth of practice samples, and helped CalTech design processing mask
- Developed top cell and 3-junction IMM devices specific for the environment of CalTech's system: AM0 spectra, 15 suns, 80 °C
- Characterized devices at various temperatures and concentrations
- Supplied 3-junction devices for irradiation
- Provided 3-junction material for processing on Kapton tape, and potentially for prototyping concentrator performance
- Developed radiation-hard GaInAsP 1.0 eV cell
- Grew and characterized 3-junction rad-hard device including GaInAsP subcell
- Grew and characterized 4-junction IMM device
- Results presented at PVSC and submitted to J. Photovoltaics by CalTech with NREL help

Task 1

Task description

Design 3J IMM structure optimized for AM0 (Air Mass = 0) spectrum at 80°C and 10 - 30X concentration (15x nominal). Cells will be compatible with epitaxial lift-off (ELO) processes but

will not be processed for growth substrate recovery. Cells will initially be grown on relatively small 2 x 2 cm active area pieces (then later, on 2" wafers), and processed into smaller cells of various designs including primarily ~1mm wide cells of varying length (up to 40mm; 10mm typ.) as well as test and/or calibration cells and structures. The target is > 32% AM0 efficiencies at 25°C 15-sun. Optimization of structure at these conditions involves modeling. Designs will be varied and/or iteratively improved based on experimental results throughout the project.

Task summary and major results

This task involved development of several new multijunction alloys and structures for possible use in the CalTech PV system, as well as the necessary device modeling. First, 3J-IMM devices specifically optimized for the CalTech system and operating conditions were developed. This device was optimized through characterization and growth iteration, and later supplied to CalTech. Then, a radiation hard 3J-IMM device was designed that uses GaInAsP for increased radiation tolerance. The GaInAsP alloy was developed, resulting in a bandgap-voltage difference Woc = 0.4 V, and incorporated into a rad-hard 3J-IMM, which was grown and characterized. Finally, a 4J-IMM device was designed to maximize efficiency while increasing the voltage for the voltage required to power the power transmission in the CalTech system. The 3J-IMM was most developed, and performed extremely well with predicted efficiency over 33% at operating conditions. One 3J-IMM rad-hard was grown, which showed that GaInAsP can be implemented into a 3J structure for increased radiation tolerance without major BOL efficiency loss. One 4J-IMM device was grown, which increased efficiency with regard to the 3J structure while providing the necessary voltage required. Table I shows results at 1 sun AM0 and 25 °C without ARC, and the detailed work is described next.

Table 1: Multijunction Cell Results at 1-sun AM0 (1366 W/m^2) and 25 °C, no ARC

	3J-IMM	3J-IMM-RadHard	4J-IMM
Voc (V)	3.095	2.970	3.345
Jsc (mA/cm^2)	12.0	11.2	11.6
FF (%)	86.6	83.4	84.2
Efficiency (%) (Estimated with ARC)	23.5 (31.5)	20.4	23.9

Detailed task work

3J-IMM device modeling

First, the optical transfer function was calculated based on the measured transmittance of the optical components at CalTech/Space Solar Power Initiative(SSPI). The optical transfer function modifies the AM0 spectrum, and allows cell modeling. CalTech's system optics do not change the spectrum from 400 nm to longer wavelengths, which means that the major modifications to

the spectrum will be related to the device window layer and anti-reflective coating (ARC), with the system adding only some small spectra change in the blue region.

Using various optical transfer functions, optimal bandgaps of the 3-junction IMM device were determined using a dark I-V model, shown in Figure 1. At the design temperature, 80 °C, the GaAs bandgap is very close to the optimal bandgap for the middle subcell. The top cell is more impacted by changes to the spectrum than the bottom cell. At the design temperature and concentration, 80 °C and 15 suns, and using the expected spectral losses described by "case 2", **the loss in efficiency by using GaAs instead of the optimal bandgap is minimal** and likely outweighed by lattice-mismatch related losses. With GaAs as the middle subcell, the optimal top cell bandgap is close to 1.9 eV, a disordered GaInP subcell, and the optimal bottom cell bandgap is around 1.0 eV. This analysis allows us to determine the necessary device development steps.

The top cell needs to be optimized for excellent current collection while maintaining a sheet resistance that leads to low shadowing at the design concentration. Front grid modeling was performed for a range of sheet resistances to determine top cell tradeoffs related to shadowing, shown in Figure 2. The model optimizes for a the current and voltage expected at 15 suns (3V, 250 mA/cm^2), with a contact resistance finger thickness, and metal resistivity that are commonly achieved in our lab: 10^{-4} ohm-cm^2, 2 μm, and 2.7 x 10^{-6} ohm-cm, respectively.

At a sheet resistance of 500 Ohm/sq, the power loss is not a strong function of finger spacing between 300 μm and 1000 μm. Devices with 1000 Ohm/sq have 1% resistive losses than those with 500 Ohm/sq at a finger spacings of 600 μm. Devices with 300 – 400 μm finger spacing and sheet resistance between 500 – 1000 ohm/sq have minimal loss. Minimizing finger width is always beneficial but not always technologically feasible, and Figure 2 (right) shows the optimal finger spacing given the limitations of the processing. The graphs in Figure 2 give input into the mask design for the concentrator system. Since the concentration factor is low, the sheet resistance demands of the top cell are not great. Tradeoffs between carrier collection and sheet resistance are likely minimal, but still require analysis.

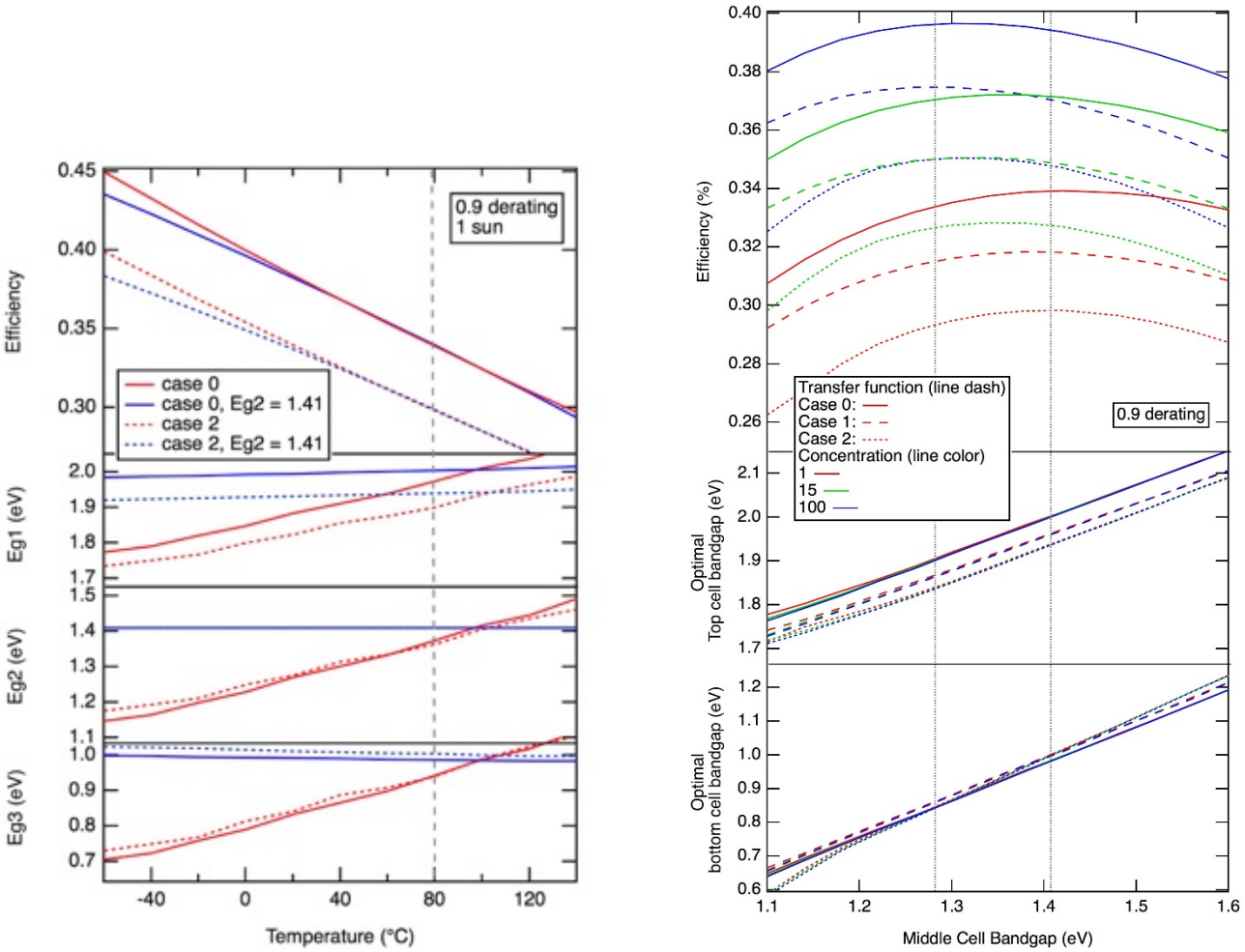

Figure 1 (left) Modeled performance and optimal bandgap combination of 3-junction devices at various temperatures and for different transfer functions. (right) Modeled performance and optimcal bandgaps of the top two subcells as a function of the bandgap of the middle subcell, for 3-junction devices at 80 °C and at various concentrations. "Case 0" uses exactly the AM0 spectrum in the model, "Case 1" modifies the AM0 spectrum for unavoidable losses in the AlInP window, and "Case 2" modifies the AM0 spectrum for both window losses and ARC losses.

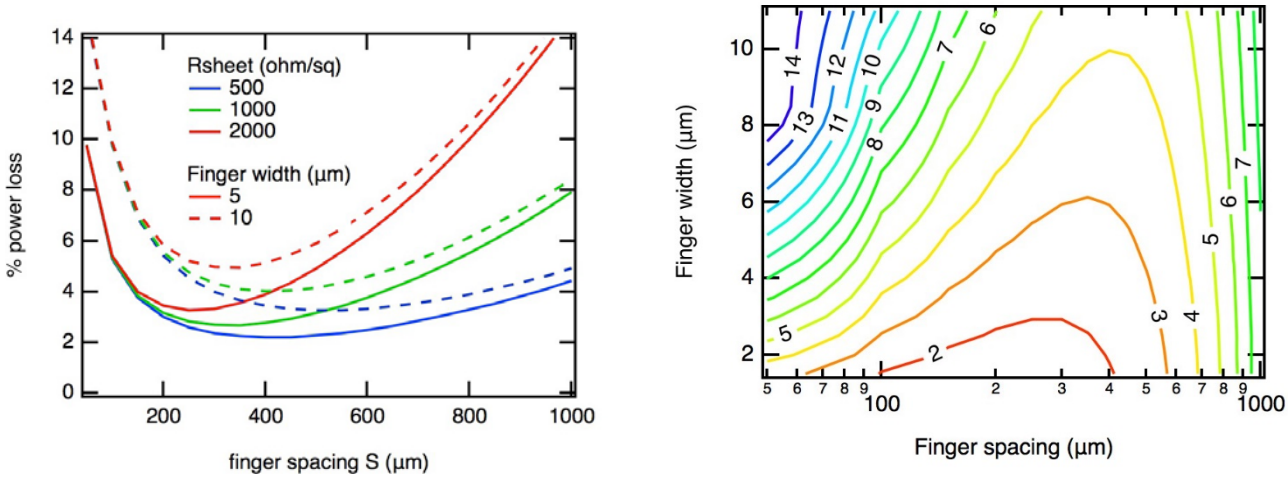

Figure 2 (left) Power loss (%) as a function of finger spacing for different finger widths and different sheet resistances. (right) Power loss (%) for a sheet resistance of 1000 Ohm/sq as a function of finger width and spacing.

GaInP top cell development

Two new GaInP top cells, MQ366 and MQ398, were compared with two top cells previously grown at NREL, MO524 and MP405 in order to optimize the top cell for this project. The bandgap, voltage, carrier collection, and sheet resistance are important considerations. These parameters are influenced by the substrate orientation, doping levels, and growth conditions, which are varied in this sample set:

MO524: 2°B GaInP, Tgrowth = 700 °C

MP405: 6°A GaInP, Tgrowth = 750 °C

MQ366: 2°B GaInP, Tgrowth = 750 °C, low emitter doping

MQ398, 2°B GaInP, Tgrowth = 750°C, high emitter doping

Results from this sample set of top cells is shown in Figure 3. High doping in the emitter tends to lower diffusion length and limit the blue response of the EQE. The loss in photocurrent is analyzed by integrating the EQE with the AM0 spectrum in the wavelength range between 375 nm – 500 nm. Only minor collection differences exist between 700 Ohm/sq and 2000 Ohm/sq, on the order of 0.1 mA/cm^2 (Figure 4, right). From the device modeling described earlier, 700 Ohm/sq also leads to low grid-related losses with a finger spacing of 500 µm, making it a good target for the sheet resistance of these top cells.

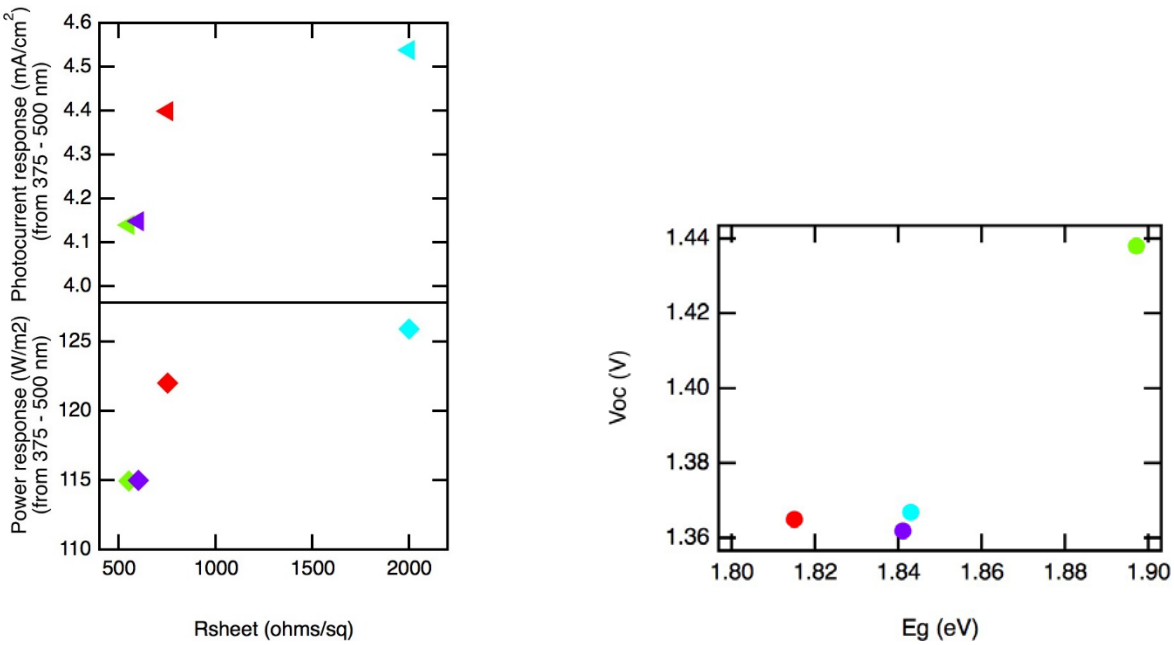

Figure 3 (left) Analysis of carrier collection tradeoffs with sheet resistance. (right) Voltage tradeoffs as a function of bandgap.

Disordered GaInP material leads to a higher bandgap and can be achieved, amongst other things, using (001) GaAs miscut towards (111)A or using high growth temperature. Here, we show that high growth temperature on a substrate miscut towards (111)B only slightly raises the bandgap, and the voltage does not improve with the increase in bandgap. However, high voltage is

achieved using high growth temperature on (111)A-miscut substrates, shown in Figure 4 (right), which are the growth conditions adopted for the 3-junction IMM device.

3-junction IMM development

The initial 3-junction IMM device uses a top cell based off MP405, but with lower emitter doping to target Rsheet = 700 Ohm/sq. The middle subcell is GaAs and the bottom subcell is 1.0 eV GaInAs. The metamorphic bugger is made of AlGaInAs, and the tunnel junctions are AlGaAs/GaAs/AlGaAs.

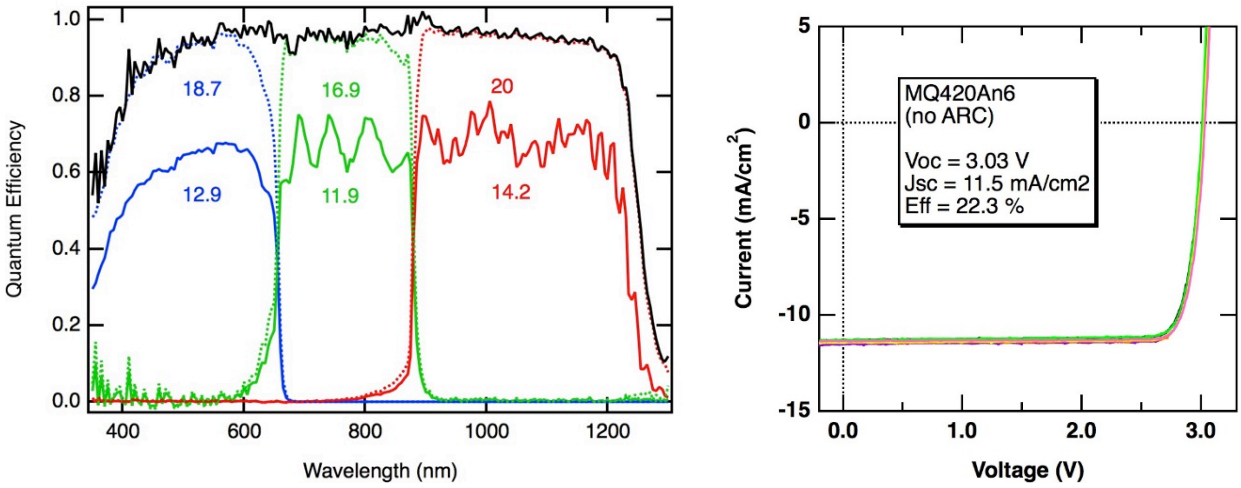

Figure 4 (left) EQE and IQE of MQ420, the initial 3-junction IMM device. Integrated currents are shown under the respective QE plateaus, and the summed IQE is shown in black. (right) 1-sun LIV results without ARC, which shows a high overall voltage and Jsc that agrees with the EQE limited by the GaAs subcell.

Figure 4 shows results from the initial 3J-IMM device. **The IQE is exceptionally high throughout all junctions**, showing very low carrier collection loss. The top cell has excess current at 25°C, and is expected to gain current with respect to the other junctions as the temperature is raised. The photocurrent thus needs rebalancing in the next design. **The voltage is high, 3.03 V**, and the EL (not shown) shows that the GaAs subcell could be further improved. No tunnel junction breakdowns occur below 800 suns (not shown).

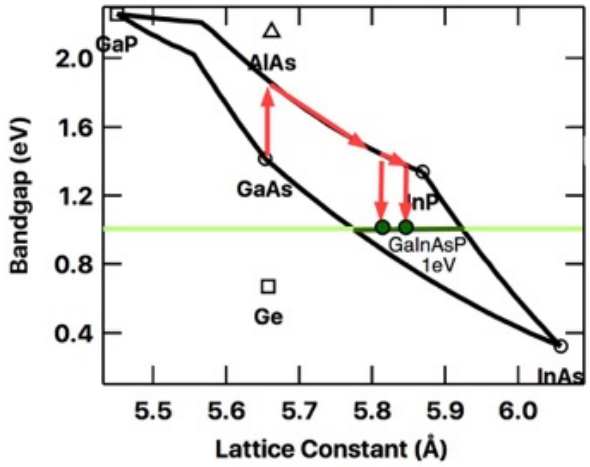

Figure 5 Bandgap vs lattice constant of binary III-V semiconductors and ternary tie-lines, sown in black. The 1.0 eV bandgap is highlighted in light green, and the GaInAsP 1.0 eV alloys are highlighted in dark green. These materials can be accessed using GaInP compositionally graded buffers on GaAs substrates, with the routes shown in red.

Several strategies to enhance radiation hardness are well known, such as altered doping profiles and subcell thinning. **Here, we investigate a new strategy: substituting 1.0 eV GaInAsP for 1.0 eV GaInAs**. A variety of quaternary 1.0 eV GaInAsP alloys with variable phophorous content are accessible using compositionally graded buffers, shown in Figure 5. Development of this new material is required.

Gas phase to solid phase incorporation of mixed group V compounds is nonlinear and highly temperature dependent, and so requires calibration. Initial calibrations were performed on GaAsP graded buffers on GaP grown at 650 °C, the expected subcell growth temperature. The solid phase composition is calculated using HR-XRD reciprocal space maps (RSMs).

The As/P incorporation curve was used to determine the appropriate As/P gas mixture for 1.0 eV GaInAsP with various phosporous contents. 1.0 eV GaInAsP cells with both 25% and 45% phosporous were attempted by modifying the graded buffer for the appropriate lattice constant (Figure 7). Initial cells (green lines) were not lattice-matched to the graded buffer, had slightly incorrect bandgaps, and performed poorly, shown in Figure 6. However, after fine-tuning the gas flows for lattice-matching and optimal bandgap, the **GaInAsP cell with 25% phosphorus content achieved a Woc = 0.4 V**. The 45% device was still not lattice-matched to the buffer, and had a Woc > 0.5 V.

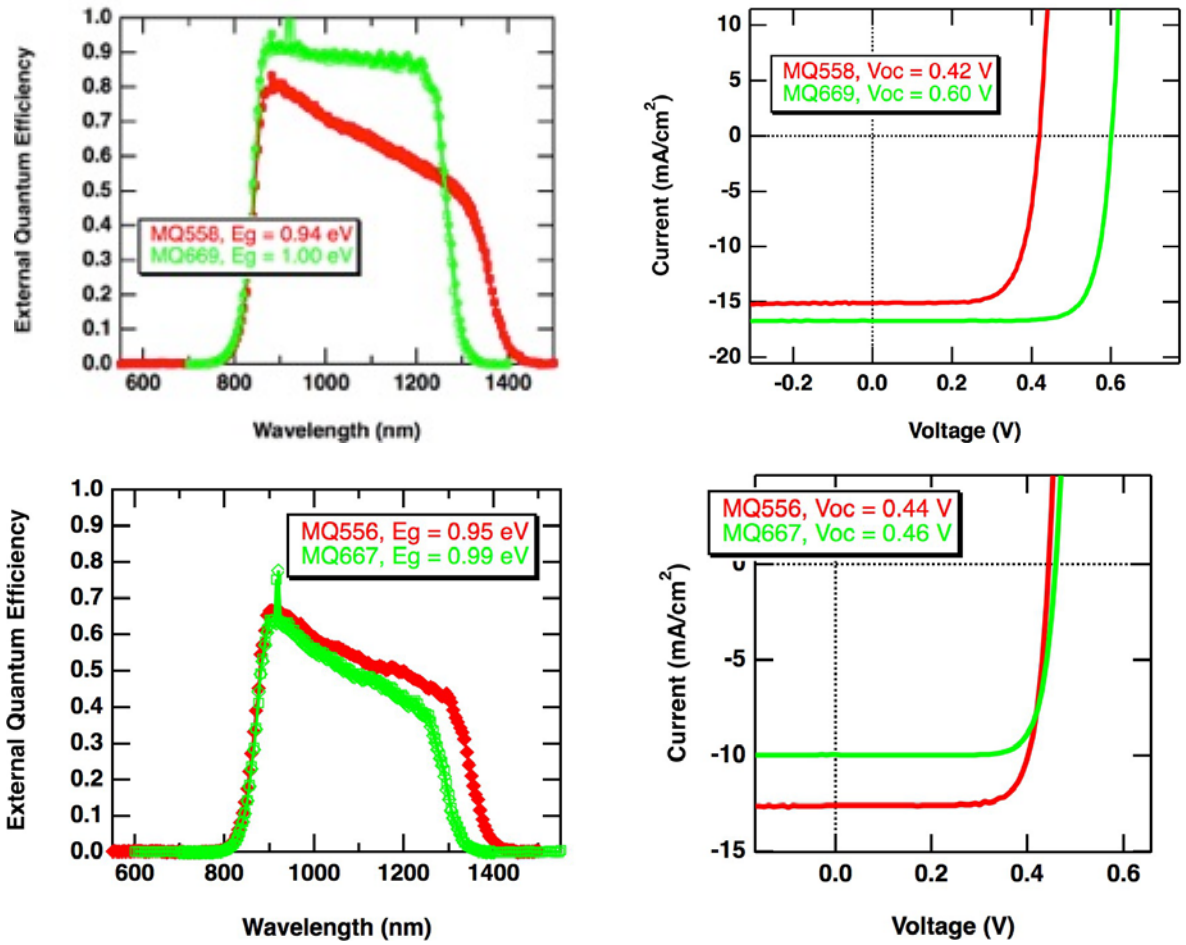

Figure 6 EQE (top left) and LIV (top right) of 1.0 eV GaInAsP with 25% phosphorus content. EQE (bottom left) and LIV (bottom right) of 1.0 eV GaInAsP with 45% phosphorus content. The green lines are the first batch of cells, and the red lines are the second batch of cells after optimizing gas flows for lattice-matching and for the correct bandgap.

3J-IMM Rad-Hard device development

One 3-junction IMM device was designed to be radiation hard by incorporating some standard radiation hardnening techniques as well as incorporating the 1.0 eV GaInAsP cell with 25% phosphorus content. The structure of the rad-hard device is compared with the standard 3J-IMM in Figure 7.

MQ463: prototype 3J-IMM

Component	Material	Bandgap (eV)	Thickness (µm)
Top cell	GaInP	1.90	0.65
Middle Cell	GaAs	1.41	2.8
Bragg Reflector	(none)		
Graded Buffer	AlGaInAs	> 1.5	4
Bottom Cell	GaInAs	1.01	2.1

MR027: Rad-Hard 3J-IMM

Component	Material	Bandgap (eV)	Thickness (µm)
Top cell	GaInP	1.89	0.5
Middle Cell	GaAs	1.42	2
Bragg Reflector	AlGaAs	> 1.5	2
Graded Buffer	GaInP	> 1.5	5.3
Bottom Cell	GaInAsP	0.99	1.5

Figure 7 Structure comparison between the standard 3J-IMM used in the prototype and the 3J-IMM designed for radiation hardness.

All subcells are thinned to improve end-of-life (EOL) Jsc. The top cell bandgap is lowered using atomic ordering to enable thinning to 0.5 μm without loss of current. A Bragg reflector is placed behind the GaAs subcell, which allows physical thinning to 2 μm while minimizing optical thinning. The GaInAsP subcell takes advantage of a Au back reflector behind the subcell, enabling thinning to 1.5 μm with minimal loss. The emitter of the first and second subcells is slightly thicker to aid EOL Jsc. Finally, and most importantly for this study, **the bottom subcell alloy is GaInAsP rather than GaInAs, which should aid EOL voltage**.

Device results are shown in Figure 8. The IQE is high for all junctions, showing that the Bragg reflector aids collection in the GaAs subcell and that there are no diffusion length problems in the GaInAP subcell. The modeled intergrated currents show that the bottom subcells have excess current with respect to the top cell, as designed. **The voltage is high, 2.97 V**, which is only slightly below the expected voltage for this bandgap combination. Some improvement is likely possible by determining subcell nonradiative recombination and finding and limiting the source of the nonradiative recombination. The most major issue with this device is a nonlinear resistance around Jsc, likely indicating an internal barrier within the semiconductor. This barrier may limit voltage and fill factor and likely adds unneccesary series resistance that limits performance at higher concentrations. Future work should initially target determining the source of this barrier. However, **there is no indication that the 1.0 eV GaInAsP subcell significantly affects the BOL device efficiency**, making it a good candidate to raise EOL efficiency.

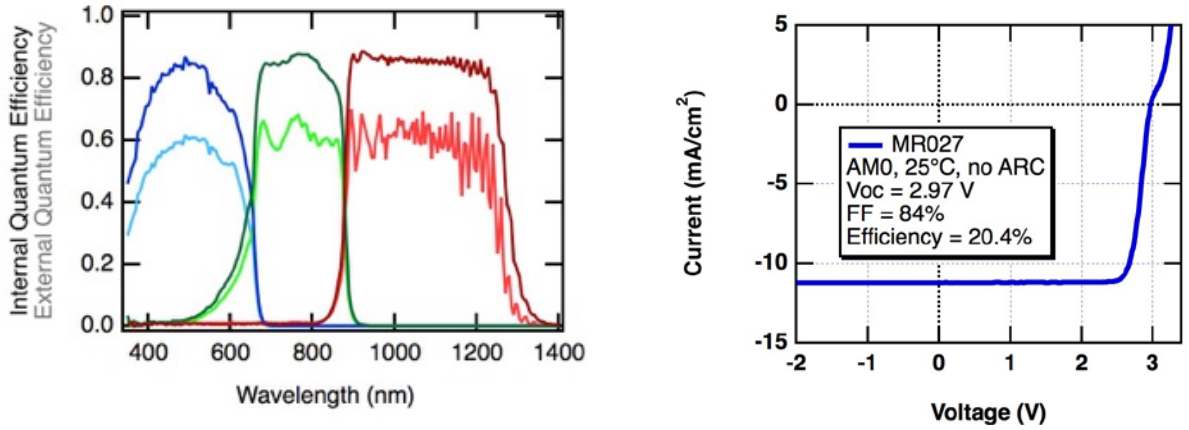

Figure 8 (left) Measured EQE and IQE of the 3J-IMM Rad-Hard. (right) LIV of the same device at 1-sun AM0, 25°C, and without ARC.

4J-IMM development and results

A 4-junction device could deliver the higher voltage required for power transmission from the CalTech space PV system, but is a more difficult structure to optimize. An initial device was designed, grown and characterized. The design is similar to the 3J-IMM with the addition of a GaInP+InSbP compositionally graded buffer to access 0.70 eV GaInAs. The device results are shown in Figure 9.

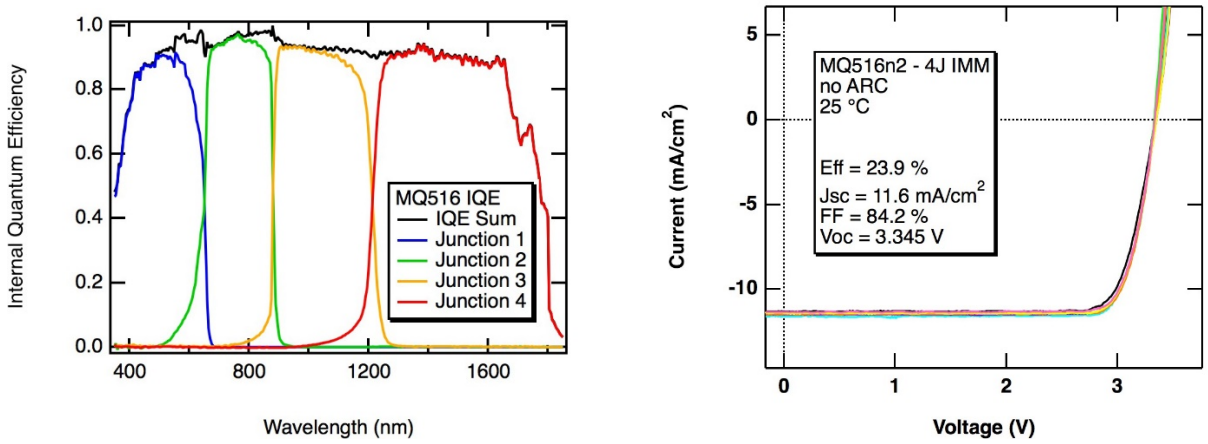

Figure 9 (left) IQE of each junction as well as the summed IQE. The longest wavelengths have a measurement artifact due to an uncalibrated QE detector. (right) LIV results from the 4J-IMM.

The EQE and IQE of the 4-junction IMM are excellent for all junctions. **The voltage is high, 3.345 V**, but could be improved with further device optimization. **These results show that the 4J-IMM can easily be tuned to provide a high efficiency while operating at the optimal voltage required by the CalTech system**.

Task 2

Task description

Produce 3J IMM solar cells as designed in Task 1.

Task summary and major results

In this task, NREL produced and supplied 3J-IMM devices for processing at CalTech onto a thin substrate, for radiation testing, and potentially for use in a concentrator prototype system. NREL taught CalTech inverted device processing during a 3-day site visit. CalTech took NREL's optimized 3J-IMM and processed it onto Kapton tape, showing extremely high specific power.

Detailed task work

MQ463 was designed based off the results from MQ420. The top cell was thinned for improved current balancing, and the middle subcell voltage was improved by using a GaInP BSF instead of AlGaAs. Results are shown in Figure 10.

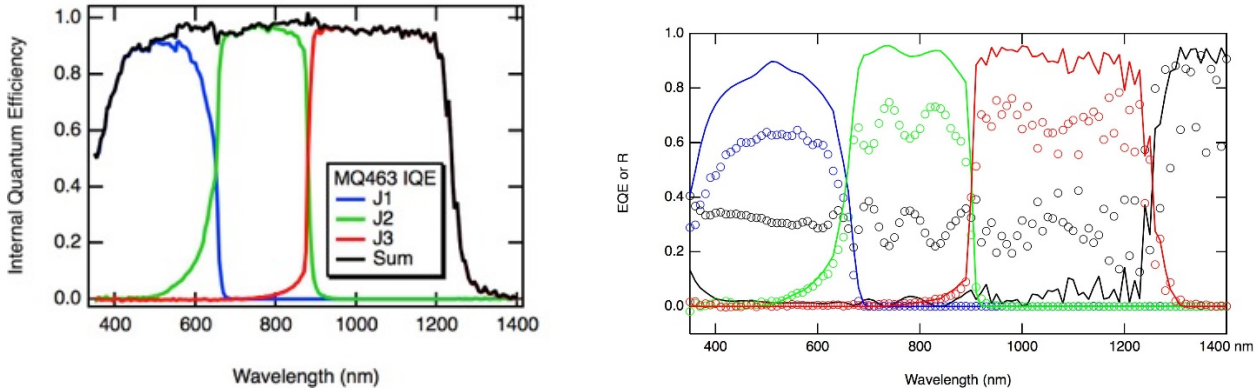

Figure 10 (left) IQE and IQE sum of the 3J-IMM device used in the prototype, measured at 25 °C. (right) Measured EQE (markers) and modeled EQE (lines) of the 3J-IMM in the prototype, measured at 80 °C.

All subcells have excellent voltage, determined by EL, and excellent carrier collection. The integrated subcell photocurrents at 80 °C for the top, middle, and bottom subcells are 17.4, 17.7, and 18.2 mA/cm^2, respectively, and so are well balanced at the operating point. No tunnel junction breakdowns occurred in this device, not shown. This growth was repeated two times, MQ474 and MQ476, and supplied to CalTech.

NREL taught CalTech the inverted device processing technique during a 3-day site visit, using several test single-junction and a 3J-IMM test samples provided by NREL. Then, CalTech processed MQ474 and MQ476 at CalTech by removing the substrate and bonding the device onto a Kapton tape handle. The weight of a 10 mm x 1 mm sample is 2 mg, compared to 15 mg for a commercial 3J cell. **Due to its high efficiency and low weight, the 3J-IMM on Kapton tape is promising for a device with very high specific power**. Results were shown in a presentation at PVSC and a submitted manuscript in J. Photovoltaics.

Task 3

Task description

Characterize cells as function of temperature between -100° and +120°C including

- Standard current-voltage (IV) and external quantum efficiency (EQE) measurements
- Measurements under low concentration 10-30X
- Perimeter recombination of long, thin (~10mm x 1mm) cells
- Electroluminescence (EL) for subcell voltage characterization with multijunction device
- Effects of radiation dose (performed elsewhere e.g. Jet Propulsion Laboratory, Aerospace Corp.)
- Effects of thermal cycling in vacuum (thermal cycling performed at Cal Tech).

Task summary and major results

In this task, NREL measured multijunction devices at various temperatures and concentrations to validite for use in CalTech's sytem. Samples performed as expected. **The optimized 3J-IMM is predicted to achieve over 33% efficiency in CalTech's system and operating conditions.** No unexpeceted losses occurred at higher temperatures, and all tunnel junctions performed well under concentrated light.

Detailed task work

3J-IMM characterization

CalTech and NREL determined that measurements around operating temperature, 80 °C, had priority over low temperature measurements. The 3J-IMM was tested between room temperature and 100 °C, and at concentrations from 1 sun to 50 suns. Results are shown in Figure 11.

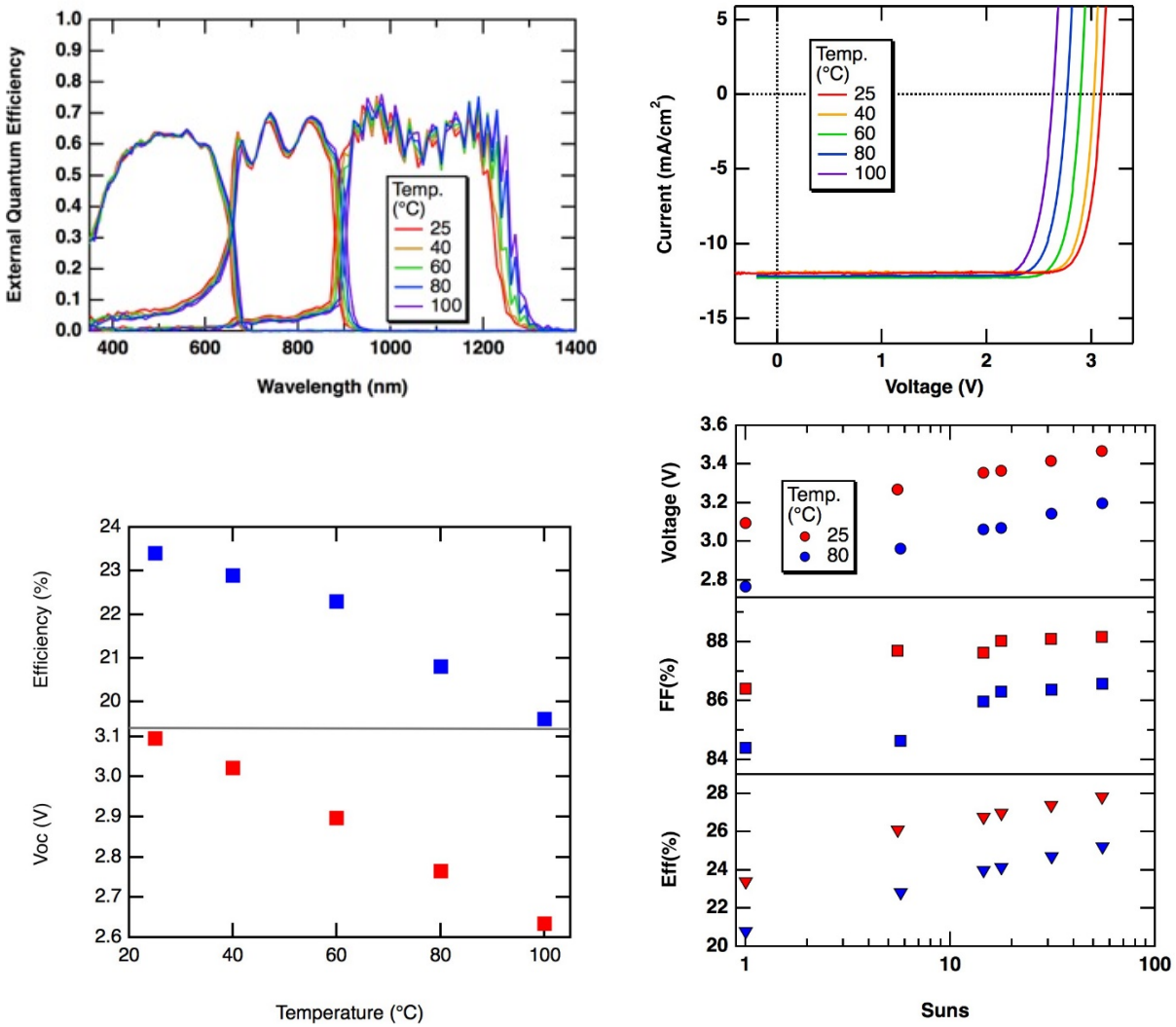

Figure 11 EQE (top left) and LIV (top right) of 3J-IMM devie measured at temperatures from 25 – 100 °C, and calculated Voc and efficiency (bottom left) from these measurements. (bottom right) Voc, FF, and efficiency at elevated illumination concentrations at both 25 °C and 80 °C.

The bandgap lowers as the temperature is increased, which is observed in Figure 11 (top left). The cell is designed for operation at 80 °C by using higher bandgaps than are optimal at room temperature. No absorption gaps exist in the AM0 spectrum, which eases the design. The FF increases with concentration up to 50 suns, which shows that all tunnel junctions are effective throughout the range surrounding the operating point, 15 suns. **No unexpected losses occurred at elevated temepratures or elevated concentration.**

These devices were sent to CalTech and irradiated at AeroSpace Corp. **Radiation degradation results were shown in a presentation at PVSC and a submitted manuscript in J. Photovoltaics**.

4J-IMM characterization

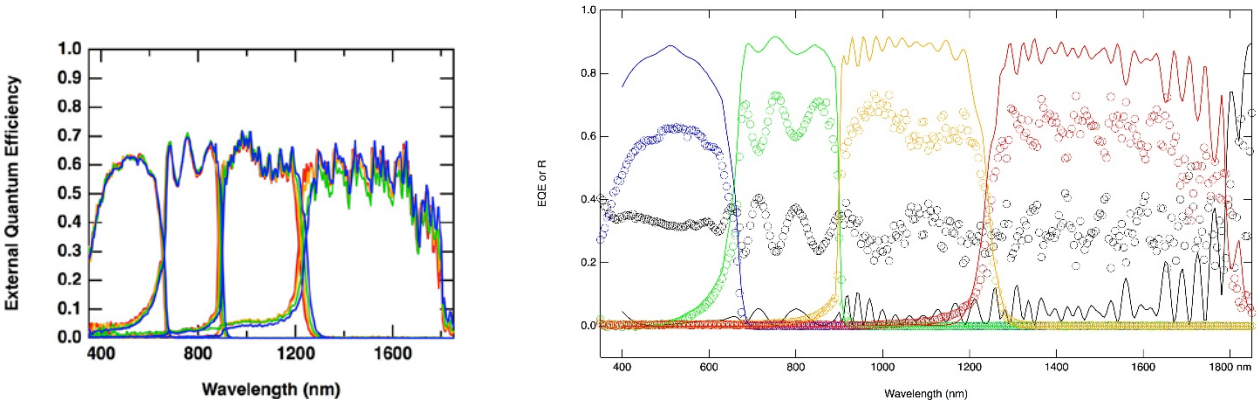

Figure 12 (left) EQE of 4J-IMM device measured at temperatures from 25 – 100 °C. A measurement artifact exists at long wavelengths (1700 - 1800 nm) due to an uncalibrated detector. (right) Measured EQE at 80 °C without an ARC (markers) and modeled EQE under coverglass and with a Al_2O_3/TiO_2 ARC at 80 °C(lines).

Initial 4J-IMM devices were also tested at elevated temperature, results shown in Figure 12. Similar to the 3J-IMM, no unexpected losses occurred. The modeled EQE at 80 °C under coverglass and with ARC showed that the subcells were very-well current balanced: J1 = 17.1, J2 = 16.8, J3 = 17.0, J4 = 17.0 mA/cm^2. This is excellent for BOL efficiency but must be altered to maximize EOL efficiency.

Subject Inventions Listing:

None

Report Date:

7/25/18

Responsible Technical Contact at Alliance/NREL:

Ryan France, ryan.france@nrel.gov

Name and Email Address of POC at Company:

Michael Kelzenberg, mdk@caltech.edu

DOE Program Office:

Office of Energy Efficiency and Renewable Energy (EERE), Solar Energy Technologies Office

This document contains NO confidential, protectable, or proprietary information.